

# Disturbing synchronization: Propagation of perturbations in networks of coupled oscillators

Damián H. Zanette

Consejo Nacional de Investigaciones Científicas y Técnicas

Centro Atómico Bariloche and Instituto Balseiro, 8400 Bariloche, Argentina

Received: date / Revised version: date

**Abstract.** We study the response of an ensemble of synchronized phase oscillators to an external harmonic perturbation applied to one of the oscillators. Our main goal is to relate the propagation of the perturbation signal to the structure of the interaction network underlying the ensemble. The overall response of the system is resonant, exhibiting a maximum when the perturbation frequency coincides with the natural frequency of the phase oscillators. The individual response, on the other hand, can strongly depend on the distance to the place where the perturbation is applied. For small distances on a random network, the system behaves as a linear dissipative medium: the perturbation propagates at constant speed, while its amplitude decreases exponentially with the distance. For larger distances, the response saturates to an almost constant level. These different regimes can be analytically explained in terms of the length distribution of the paths that propagate the perturbation signal. We study the extension of these results to other interaction patterns, and show that essentially the same phenomena are observed in networks of chaotic oscillators.

**PACS.** 05.45.Xt Synchronization; coupled oscillators – 05.65.+b Self-organized systems

## 1 Introduction

Synchronization is a paradigmatic mode of emergent collective behaviour in ensembles of interacting dynamical elements [1,2]. It arises in a broad class of real systems, com-

prising from mechanical and physico-chemical processes [3,4,5] to biological phenomena [6,7,8], and is reproduced by a variety of mathematical models. Roughly speaking, it consists of some kind of coherent evolution where the motions of individual elements are correlated in time. De-

pending on the nature of the individual dynamical laws and on the interactions, different forms of synchronized states are possible. They range from full synchronization, where all the elements follow the same orbit in phase space, to weakly correlated forms where the ensemble splits into almost independent clusters of mutually synchronized elements, or where coherence manifests itself in just a few state variables or in time averages of suitably chosen quantities [9,2]. Full synchronization is typical for globally coupled ensembles of identical elements, where any two elements interact with the same strength. When coupling is strong enough and represents an attractive interaction, the asymptotic state where all elements share the same orbit is stable [10]. Under certain conditions, stability of the fully synchronized state can also be insured for more complex interaction patterns, where each pair of elements may or may not interact [11]. Weaker forms of synchronization are characteristic of ensembles of non-identical dynamical elements.

A simple but quite useful model for an ensemble of coupled dynamical elements is given by a set of  $N$  phase oscillators, whose individual dynamics in the absence of coupling is governed by  $\dot{\phi} = \omega$ . The phase  $\phi(t) \in [0, 2\pi)$  rotates with constant frequency  $\omega$ . This elementary representation of periodic motion, originally introduced as a model for biological oscillations [7], approximates any cyclic dynamics, even in the presence of weak coupling [9]. As for the interaction pattern, it can be thought of as a graph, or network, with one oscillator at each node. The graph is characterized by its adjacency matrix  $\mathcal{J} = \{J_{ij}\}$ .

If oscillator  $i$  is coupled to oscillator  $j$ , i. e. if the phase  $\phi_j(t)$  enters the equation of motion of  $\phi_i(t)$ , we have  $J_{ij} = 1$ , and  $J_{ij} = 0$  otherwise. The adjacency matrix is not necessarily symmetric and, thus, coupling is not always bidirectional. In other words, the interaction network is generally a directed graph. The coupled oscillator ensemble is governed by the equations [12]

$$\dot{\phi}_i = \omega_i + k \sum_{j=1}^N J_{ij} \sin(\phi_j - \phi_i) \quad (1)$$

for  $i = 1, \dots, N$ , where  $k$  is the coupling strength. The case of global coupling,  $J_{ij} = 1$  for all  $i$  and  $j$ , has been studied in the thermodynamical limit by Kuramoto [9], who found that, as the coupling strength grows, the system undergoes a transition to a state of frequency synchronization, as first predicted by Winfree [13]. The transition parameters are determined by the distribution of natural frequencies  $\omega_i$ .

For identical oscillators,  $\omega_i = \omega$  for all  $i$ , and for all  $k > 0$ , the long-time asymptotic state of a globally coupled ensemble is full synchronization. More generally, it is possible to show that full synchronization is stable when the interaction network is regular, i. e. when all oscillators are coupled to exactly the same number  $z$  of neighbours [11]. In this situation,  $\sum_j J_{ij} = z$  for all  $i$ .

A fully synchronized oscillator ensemble can be thought of as an active medium in a rest-like state. Microscopically, this stable state is sustained by the highly coherent collective dynamics of the interacting oscillators. A key feature characterizing the dynamical properties of the medium is determined by its response to an external perturbation. How is the synchronized state altered as the perturbation signal propagates through the ensemble? Which propaga-

tion properties does coupling between oscillators establish in the medium? The effect of external forces on ensembles of interacting dynamical systems has been studied in detail for global coupling, both for periodic oscillators and chaotic elements [14,15,16,17]. Ordered oscillator arrays have also been considered [18]. The above questions, however, are especially significant for more complex interaction patterns—in particular, for random interaction networks—where the non-trivial geometric structure is expected to play a relevant role in the propagation process. Quite surprisingly, the problem seems to have been addressed for the first time only recently [19,20].

In this paper, we present numerical calculations and analytical results for the propagation of a perturbation in an ensemble of identical phase oscillators, governed by the equations

$$\dot{\phi}_i = \sum_{j=1}^N J_{ij} \sin(\phi_j - \phi_i) + a\delta_{i1} \sin(\Omega t - \phi_i). \quad (2)$$

Without generality loss, the natural frequency of oscillators and the coupling strength are fixed to  $\omega = 0$  and  $k = 1$ , respectively. The external perturbation is represented by an additional oscillator of constant frequency  $\Omega$ , to which a single oscillator in the ensemble—i. e., oscillator 1—is coupled with strength  $a$ . To take advantage of certain analytical results regarding regular graphs, we take a connection network where each oscillator is coupled to exactly  $z$  neighbours. Our main goal is to relate the response of the ensemble to the metric properties of the interaction network. In particular, we pay attention to the dependence on the distance to the node where the perturbation is applied, and on the perturbation frequency.

The paper is organized as follows. In the next section, we present numerical results for random interaction networks of phase oscillators. We show that the system response is, essentially, a resonance phenomenon, and identify two regimes in the dependence on the distance. In Sect. 3, we reproduce the numerical results through an analytical approach in the limit of small-amplitude perturbations. We propose an approximation to obtain explicit expressions which clarify the role of the network structure in the propagation process. In Sect. 4, we extend our results to other geometries, including ordered networks with uni- and bidirectional interactions and hierarchical structures. Moreover, we show that the same propagation properties are observed in networks of chaotic oscillators, which broadly generalizes our conclusions. Results are summarized and commented in the final section.

## 2 Numerical results

We have solved Eqs. (2) numerically, for an ensemble of  $N = 10^3$  oscillators. We have considered a random regular network, with  $z = 2$ . The network was constructed by choosing at random the  $z$  neighbours of each node. Multiple directed links between any two nodes were avoided, and realizations which produced disconnected networks were discarded. Most of the results presented here correspond to a perturbation of amplitude  $a = 10^{-3}$  and various frequencies, typically ranging from  $\Omega \sim 10^{-2}$  to 10. The integration  $\Delta t$  in our numerical algorithm was chosen such that  $\Omega^{-1} \gg \Delta t$ .

The ensemble was prepared in the state of full synchronization, with  $\phi_i = \phi_j$  for all  $i$  and  $j$ . Before recording the evolution of the phases  $\phi_i$ , an interval much longer than  $\Omega^{-1}$  was left to elapse. After this interval, any transient behaviour due to the combined effect of the dissipative mechanisms inherent to the coupled oscillator dynamics and the external perturbation had relaxed and the system had reached a regime of steady evolution. Numerical results show that, in this regime, each phase  $\phi_i(t)$  oscillates around the average  $\bar{\phi}(t) = N^{-1} \sum_i \phi_i(t)$ , seemingly with harmonic motion of frequency  $\Omega$ . Our aim was to quantitatively characterize the departure from full synchronization due to the response to the external perturbation. As a measure of this departure for each individual oscillator  $i$ , we considered the time-averaged mean square deviation in  $\phi$ -space, defined as

$$\sigma_{\phi_i} = [\langle (\phi_i - \bar{\phi})^2 \rangle]^{1/2}, \quad (3)$$

where  $\langle \cdot \rangle$  denotes time averages over sufficiently long intervals. The mean square deviation  $\sigma_{\phi_i}$  is a direct measure of the amplitude of the motion of each phase with respect to the average  $\bar{\phi}$ . In the fully synchronized state,  $\sigma_{\phi_i} = 0$  for all  $i$ .

It turns out that, for a given realization of the interaction network and a fixed value of the frequency  $\Omega$ ,  $\sigma_{\phi_i}$  has a rather well defined dependence on the distance  $d_i$  from oscillator 1, where the external perturbation is applied, to oscillator  $i$ . The distance  $d_i$  is defined as the number of links along the shortest directed path starting at oscillator 1 and ending at  $i$ . On the other hand, especially for large distances  $d_i$ ,  $\sigma_{\phi_i}$  may strongly depend on the specific

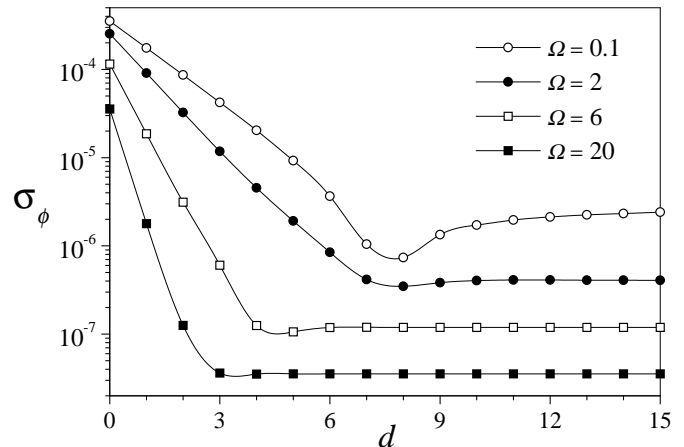


**Fig. 1.** Mean square deviation from full synchronization as a function of the distance from the oscillator where the external perturbation is applied, for various values of the frequency  $\Omega$ . As a guide to the eye, spline interpolations are shown as curves.

realization of the interaction network. In view of the well defined dependence of the mean square deviation on the distance, and for clarity in the notation, from now on we drop the index  $i$  which identifies individual oscillators.

Figure 1 shows results for the mean square deviation  $\sigma_{\phi}$  as a function of the distance  $d$  for several frequencies  $\Omega$  and a fixed interaction network. In this realization of the network, the maximal distance between oscillator 1 and any other oscillator is  $d_{\max} = 15$ . For each value of  $d$ , the individual values of  $\sigma_{\phi}$  have been averaged over all the oscillators at that distance from oscillator 1. It is apparent that the mean square deviation exhibits two well differentiated regimes as a function of the distance. For small  $d$ ,  $\sigma_{\phi}$  decreases exponentially, at a rate that sensibly depends on the frequency  $\Omega$ . In this regime, the perturbation is increasingly damped as it propagated through the system. At large distances, on the other hand,  $\sigma_{\phi}$  is practically in-

dependent of  $d$ . It is this large-distance value of  $\sigma_\phi$  which, typically, shows considerable variations between different realizations of the interaction network. The transition between the two regimes is mediated by a zone where  $\sigma_\phi$  attains a minimum, which is sharper for smaller frequencies. Thus, the mean square deviation varies non-monotonically with the distance.

The dependence of  $\sigma_\phi$  on the frequency  $\Omega$  for fixed distance reveals that the response of the oscillator ensemble to the external perturbation is, essentially, a resonance phenomenon. In Fig. 2 we plot  $\sigma_\phi$  as a function of  $\Omega$  for three values of  $d$ . For small and large distances, the mean square deviation from full synchronization displays a symmetric peak around the natural frequency of the individual oscillators ( $\omega = 0$ ). This shows that the response of the ensemble is maximal when the external perturbation varies with the same frequency of the elementary components of the system. For intermediate distances, however, an anomaly appears. While for large frequencies the response decreases as expected, the resonance peak is replaced by a local minimum at  $\Omega = \omega$ . The response is now maximal at two symmetric values around the natural frequency of the oscillators. This anomaly is directly related to the fact that the minimum in  $\sigma_\phi$  for intermediate distances (Fig. 1) is sharp for small  $\Omega$  and becomes much less distinct as the frequency of the external perturbation increases. This effect, combined with the overall decrease of  $\sigma_\phi$  as  $\Omega$  grows, implies a non-monotonic dependence  $\Omega$  at such distances, which results into the appearance of the double peak.

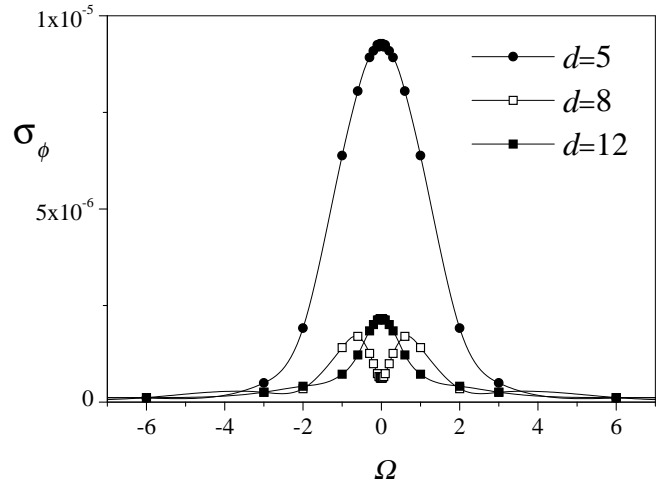


**Fig. 2.** Mean square deviation from full synchronization as a function of the frequency of the external perturbation, at various distances from the node at which the perturbation is applied. Curves, added for clarity, are spline interpolations.

The double-logarithmic plot of Fig. 3 reveals the large- $\Omega$  behaviour of the mean square deviation from full synchronization. Beyond the resonance zone,  $\sigma_\phi$  decreases with the frequency as  $\Omega^{-1}$  for all distances. Note, however, that the value of  $\sigma_\phi$  in the large- $\Omega$  regime is the same for all  $d > 0$ , while for  $d = 0$  –i. e., at oscillator 1, where the external perturbation is applied–  $\sigma_\phi$  is three orders of magnitude larger.

The fact that the mean square deviation  $\sigma_\phi$  shows a well defined dependence on the distance does not necessarily imply that the individual motions of oscillators with the same value of  $d$  are related in any specific way. As a matter of fact, being a time average,  $\sigma_\phi$  bears no information about possible correlations between the instantaneous state of different oscillators. To detect such correlations we have inspected successive snapshots of the set of individual phases plotted on the unit circle, i. e. on the plane

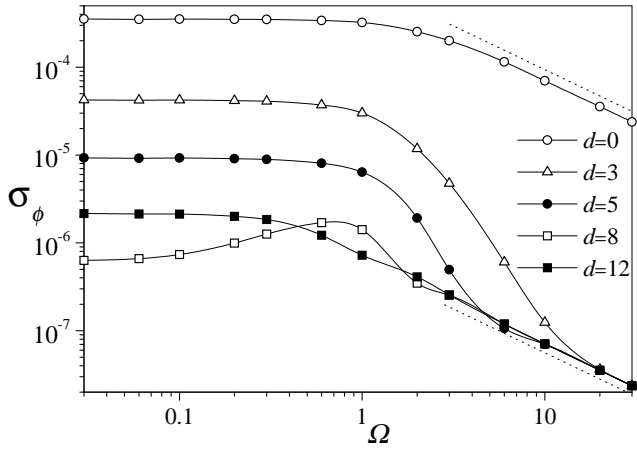


**Fig. 3.** The same as in Fig. 2, in log-log scale. Data for  $d = 0$  and  $d = 3$  are also shown. Dotted lines have slope  $-1$ .

$(\cos \phi, \sin \phi)$ . Figure 4 shows one of these snapshots for the same system of Figs. 1 to 3. It turns out that, actually, there is a strong correlation between the positions of oscillators with the same value of  $d$ . According to their distance, they form clusters of gradually decreasing deviations and growing dispersion. Clusters with  $d < 4$  are so compact that they cannot be resolved into single elements in the scale of the main plot of Fig. 4. For larger distances, clusters are relatively more disperse, as shown in the insert. Clustering in the distribution of phases reveals that, for a given value of  $d$ , oscillations around the average phase  $\bar{\phi}$  occur coherently. In the next section we show analytically that, in fact, these oscillations are very approximately in-phase.

Finally, we have studied the dependence of the response of the system on the perturbation amplitude  $a$ . Over a wide range, the mean square deviation of individual oscillators results to be proportional to the amplitude,  $\sigma_\phi \propto a$ . As an illustration, Fig. 5 shows the ratio  $\sigma_\phi/a$  as

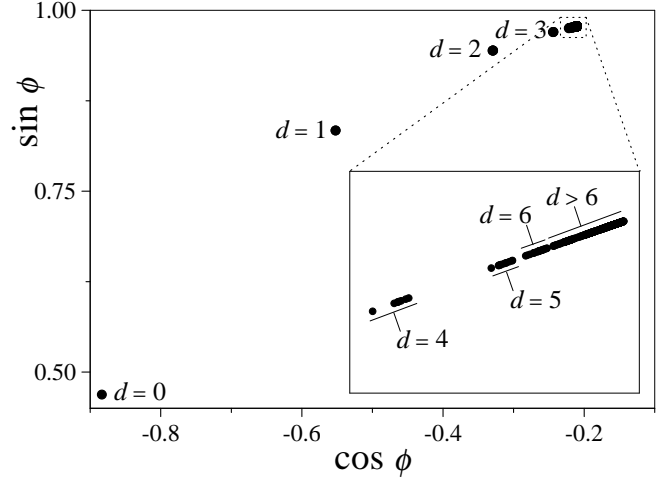


**Fig. 4.** Snapshot of individual phases on the plane  $(\cos \phi, \sin \phi)$ . Labels indicate the distance to the oscillator where the external perturbation is applied. The insert shows a close-up of oscillators with  $d > 3$ , revealing the fine cluster structure for larger distances.

a function of the distance for a perturbation frequency  $\Omega = 0.1$ . Curves collapse for all  $a \lesssim 2$ . Only for  $a > 2$  do we find significant departures from the small-amplitude regime. For  $a = 3$  the response of the whole system is relatively increased, especially, for intermediate and large distances. Finally, for  $a = 10$  we have an overall saturation of the response, and the ratio  $\sigma_\phi/a$  decreases.

In the next section, we show that most of the numerical results presented here can be analytically explained by means of a small-amplitude approximation of Eq. (2). Our analytical approach reveals the role of the interaction structure in the response of the system to the external perturbation.

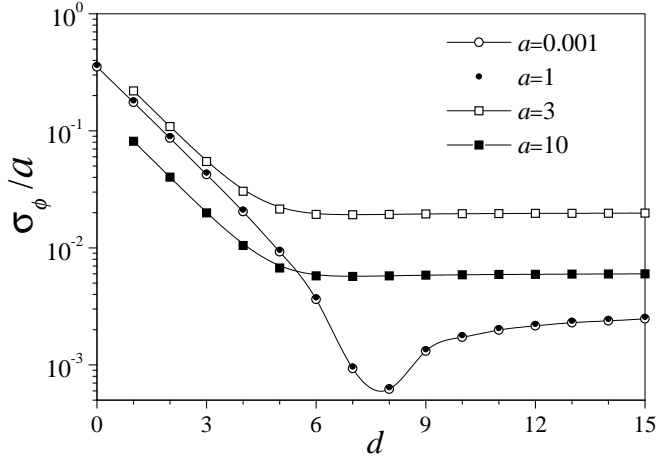


**Fig. 5.** Normalized mean square deviation,  $\sigma_\phi/a$ , for various values of the perturbation amplitude  $a$ , as a function of the distance to the oscillator where the external perturbation is applied. The perturbation frequency is  $\Omega = 0.1$ .

### 3 Analytical results

#### 3.1 Small-amplitude limit

The numerical results presented in Fig. 5 suggest that the limit of small external perturbation ( $a \ll 1$ ) bears significant information on a wide range of values for the amplitude  $a$ . It is therefore worthwhile to study this limit analytically, representing the instantaneous state of the oscillator ensemble as a perturbation of order  $a$  to full synchronization. Introducing, as in the previous section, the average phase  $\bar{\phi}(t) = N^{-1} \sum_i \phi_i(t)$ , we write the phase of oscillator  $i$  as a perturbation of order  $a$  to  $\bar{\phi}$ ,

$$\phi_i(t) = \bar{\phi}(t) + a\psi_i(t), \quad (4)$$

with  $\sum_i \psi_i = 0$ . In turn, the average  $\bar{\phi}$  is expected to vary around a constant phase  $\phi_0$ , with fluctuations of amplitude proportional to  $a$ :

$$\bar{\phi}(t) = \phi_0 + a\Phi(t). \quad (5)$$

Without generality loss, we take  $\phi_0 = 0$ .

Replacing Eqs. (4) and (5) in (2), and expanding to the first order in the perturbation amplitude  $a$ , we get

$$\dot{\Phi} = \frac{1}{N} \sum_{ij} J_{ij}(\psi_j - \psi_i) + \frac{1}{N} \exp(i\Omega t) \quad (6)$$

for the average phase deviation, and

$$\dot{\psi}_i = -\dot{\Phi} + \sum_j J_{ij}(\psi_j - \psi_i) + \delta_{i1} \exp(i\Omega t) \quad (7)$$

for the individual deviations. For simplicity in the mathematical treatment, we have replaced  $\sin(\Omega t)$  by  $\exp(i\Omega t)$ . Focusing on the case where each oscillator is coupled to exactly  $z$  neighbours, the above equations can be simplified taking into account that  $\sum_j J_{ij}(\psi_j - \psi_i) = -z\psi_i + \sum_j J_{ij}\psi_j$  and  $\sum_{ij} J_{ij}(\psi_j - \psi_i) = \sum_{ij} J_{ij}\psi_j$ .

Note that the time derivative of the average phase deviation  $\dot{\Phi}$  enters the equation of motion for the individual deviations  $\psi_i$ , Eq. (7), as a kind of external force acting homogeneously over the whole ensemble. According to Eq. (6), this effective force is of order  $N^{-1}$ . As we show later, it dominates the response of oscillators at large distances, where the effect of the perturbation signal propagated through the network is lower.

Equation (7) admits solutions of the form  $\psi_i(t) = A_i \exp(i\Omega t)$ , corresponding to steady harmonic motion at the frequency of the external perturbation. These steady solutions are expected to represent the motion once transients have elapsed. The complex amplitudes  $A_i$  satisfy a set of linear equations, which can be cast in matrix form as

$$\mathcal{L}\mathbf{A} = \mathbf{b}, \quad (8)$$

with  $\mathbf{A} = (A_1, A_2, \dots, A_N)$ . The elements of the matrix  $\mathcal{L}$  and of the vector  $\mathbf{b}$  are, respectively,

$$L_{ij} = (z + i\Omega)\delta_{ij} - J_{ij} + \frac{1}{N} \sum_k J_{kj} \quad (9)$$

and

$$b_i = \delta_{i1} - \frac{1}{N}. \quad (10)$$

For a given interaction network, the amplitudes  $\mathbf{A} = \mathcal{L}^{-1}\mathbf{b}$  can be found, for instance, numerically. Note that the amplitude modulus  $|A_i|$  is a direct measure of the mean square deviation  $\sigma_{\phi_i}$ , introduced in Sect. 2 to quantitatively characterize the departure from full synchronization in the numerical realization of our system. In fact, for harmonic motion,  $\sigma_{\phi_i} = a|A_i|/\sqrt{2}$ . The phase  $\varphi_i$  of the complex amplitude  $A_i = |A_i|\exp(i\varphi_i)$  measures the phase shift of the oscillations of  $\psi_i(t)$  with respect to the external perturbation.

Figure 6 shows the amplitude moduli  $|A_i|$  obtained from the numerical solution of Eq. (8), for an ensemble of  $N = 10^3$  oscillators with the same interaction network as in the results presented in Sect. 2. The values of  $|A_i|$  are averaged over all the oscillators at a given distance  $d$  from oscillator 1, and the subindex  $i$  is accordingly dropped. Results are presented for several values of the frequency  $\Omega$ . Dotted lines are spline approximations of the numerical data for  $\sigma_{\phi}$  already presented in Fig. 1, multiplied by a factor  $\sqrt{2}/a$ . The agreement with the solution of Eq. (8) is excellent.

The phase shifts  $\varphi_i$  corresponding to the same solutions of Eq. (8) are shown in Fig. 7, as a function of the distance and for several values of the frequency  $\Omega$ . Data for

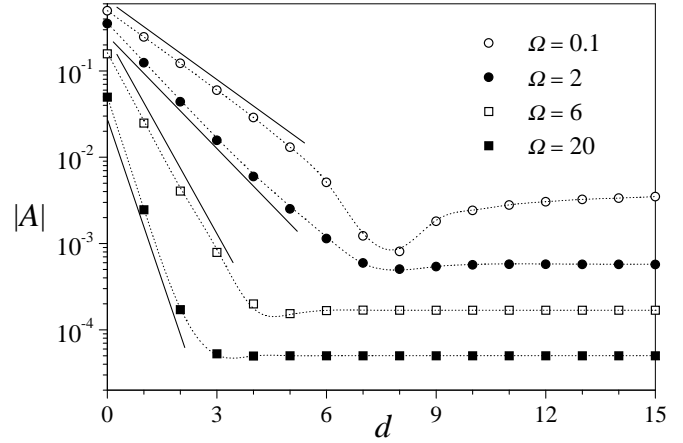


**Fig. 6.** Amplitude moduli from the numerical solution of Eq. (8), for the same system as in Fig. 1. Dotted lines are spline approximations for  $\sqrt{2}\sigma_{\phi}/a$ , for the values of the mean square deviation  $\sigma_{\phi}$  presented in Fig. 1. Full straight lines show the analytical prediction for the slope at small distances, Eq. (16).

$\Omega = 1$  are also shown. As it may be expected, phase shifts are always negative, indicating a delay in the response of the system to the external perturbation. Coinciding with the regime where the amplitude moduli  $|A_i|$  decrease exponentially, we find a zone where phase shifts vary linearly with distance. Namely, the phase shift between oscillators whose distances to oscillator 1 differ by one is a constant  $\Delta\varphi$ . This unitary phase shift, which gives the slope of  $\varphi$  as a function of the distance, depends on the frequency  $\Omega$ . In this zone, individual phases vary with distance as  $\psi_i \propto \exp[i(d_i\Delta\varphi + \Omega t)]$ . Thus, the perturbation propagates through the system at constant speed  $|\Omega/\Delta\varphi|$ . For larger distances, this linear regime breaks down, and the variation of  $\varphi$  with  $d$  tends to be much less pronounced. In the transition between both regimes, however, the phase



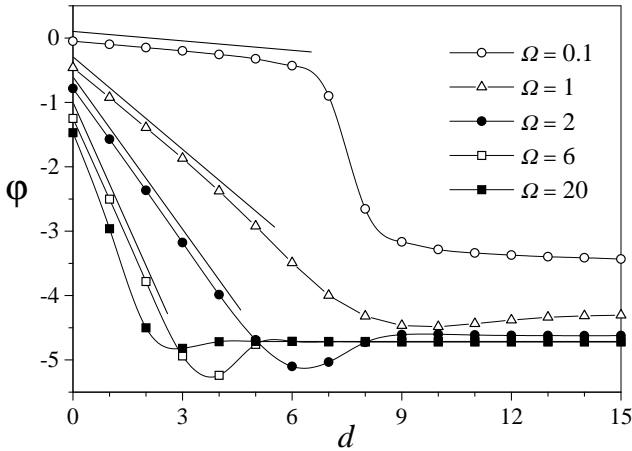


**Fig. 7.** Phase shift as a function of distance, from the numerical solution of Eq. (8) and for the same system as in Fig. 1. Straight lines show the analytical prediction for the slope at small distances, Eq. (16).

shift varies rather abruptly for small frequencies, while it develops a minimum for larger  $\Omega$ .

The results presented in Figs. 6 and 7 were obtained from the numerical solution of the small-amplitude limit equation (8). A more explicit solution can be obtained from a suitable approximation of Eq. (8), taking into account specific mathematical properties of the matrix  $\mathcal{L}$ , as we show in the following section.

### 3.2 Approximate solution

According to Eq. (9), the matrix  $\mathcal{L}$  can be written as

$$\mathcal{L} = (z + i\Omega)\mathcal{I} - \tilde{\mathcal{J}}, \quad (11)$$

where  $\mathcal{I}$  is the  $N \times N$  identity matrix, and the elements of  $\tilde{\mathcal{J}}$  are

$$\tilde{J}_{ij} = J_{ij} - \frac{1}{N}\xi_j, \quad (12)$$

with  $\xi_j = \sum_k J_{kj}$ . Our approximation to the solution of Eq. (8) is based on the following remarks.

(i) Due to the fact that  $\sum_j J_{ij} = z$  for all  $i$ , the eigenvalues of the adjacency matrix  $\mathcal{J}$  are all less than or equal to  $z$  in modulus [11]. Moreover, the eigenvalues of  $\tilde{\mathcal{J}}$  are the same as those of  $\mathcal{J}$ . In fact, if  $\mathbf{v} = (v_1, v_2, \dots, v_N)$  is an eigenvector of  $\mathcal{J}$ , then  $\tilde{\mathbf{v}} = (\tilde{v}_1, \tilde{v}_2, \dots, \tilde{v}_N)$ , with  $\tilde{v}_i = v_i - N^{-1}\sum_k v_k$ , is an eigenvector of  $\tilde{\mathcal{J}}$  with the same eigenvalue. This implies that, for  $\Omega \neq 0$ , the inverse of the matrix  $\mathcal{L}$  can be expanded as

$$\mathcal{L}^{-1} = \frac{[\mathcal{I} - (z + i\Omega)^{-1}\tilde{\mathcal{J}}]^{-1}}{(z + i\Omega)} = \sum_{m=0}^{\infty} \frac{\tilde{\mathcal{J}}^m}{(z + i\Omega)^{m+1}}, \quad (13)$$

because all the eigenvalues of the matrix  $(z + i\Omega)^{-1}\tilde{\mathcal{J}}$  are less than unity in modulus.

(ii) While  $\sum_j J_{ij} = z$  for all  $i$ ,  $\sum_k J_{kj} = \xi_j$  varies with  $j$ . Note that  $\xi_j$  is the number of links starting at  $j$ , and thus gives the number of oscillators which are coupled to oscillator  $j$ . For any realization of the interaction network, however, the average value of  $\xi_j$  over the whole ensemble is always the same,  $N^{-1}\sum_j \xi_j = N^{-1}\sum_{jk} J_{kj} = z$ . This suggests that, as an approximation to Eq. (12) avoiding the explicit calculation of  $\xi_j$ , we can take  $\tilde{J}_{ij} = J_{ij} - z/N$ . More generally, it is possible to show that this same approximation yields, for the powers of  $\tilde{\mathcal{J}}$ ,

$$\tilde{J}_{ij}^{(m)} = J_{ij}^{(m)} - \frac{z^m}{N}, \quad (14)$$

where  $J_{ij}^{(m)}$  and  $\tilde{J}_{ij}^{(m)}$  are elements of the matrices  $\mathcal{J}^m$  and  $\tilde{\mathcal{J}}^m$ , respectively.

Combining Eqs. (13) and (14), the approximate form of matrix  $\mathcal{L}^{-1}$  can be applied to the vector  $\mathbf{b}$  in the right-hand side of Eq. (8) to give the following approximation

for the amplitudes:

$$\begin{aligned} A_i &= \sum_{m=0}^{\infty} \frac{1}{(z + i\Omega)^{m+1}} \left[ J_{i1}^{(m)} - \frac{z^m}{N} \right] \\ &= \sum_{m=0}^{\infty} \frac{J_{i1}^{(m)}}{(z + i\Omega)^{m+1}} + \frac{i}{N\Omega}. \end{aligned} \quad (15)$$

In this approximation, the effect of the average deviation from full synchronization –which, as we discussed in Sect. 3.1, can be interpreted as an external effective force acting over all the oscillators with the same intensity– is represented by the terms of order  $N^{-1}$ .

It is interesting that the approximation (15) involves explicitly the matrix elements of the powers of  $\mathcal{J}$ . The matrices  $\mathcal{J}^m$  ( $m = 1, 2, \dots$ ) bear information about the metric structure of the interaction network. Specifically, the element  $J_{ij}^{(m)}$  equals the total number of directed paths of length  $m$  starting at node  $j$  and ending at node  $i$  [21]. In other words,  $J_{ij}^{(m)}$  gives the number of different ways of reaching node  $i$  from node  $j$  in exactly  $m$  steps along directed links. Equation (15) shows that the response of any individual oscillator to the external perturbation, measured by the amplitude  $A_i$ , is directly related to the number of paths through which the perturbation signal can flow from oscillator 1. Note that  $J_{i1}^{(m)} = 0$  for  $m < d_i$  and  $J_{i1}^{(m)} = 1$  for  $m = d_i$ . For oscillator  $i$ , therefore, the first contribution to the sum in the second line of Eq. (15) comes from the term with  $m = d_i$ . For  $m > d_i$ ,  $J_{i1}^{(m)}$  is different from zero if at least one path of length  $m$  starts at oscillator 1 and ends at  $i$ .

For nodes at small distances from oscillator 1, there is typically only one path of length  $d_i$  from 1 to  $i$ . In fact, the probability of having more than one path of short

length between any two oscillators is, at most, of order  $z/N$  (which we assume to be a small parameter, as in our numerical analysis). As a result, for most oscillators at a small distance from oscillator 1, we have  $J_{i1}^{(d_i)} = 1$ . Moreover, the total number of nodes with small  $d_i$ ,  $n(d_i) \sim z^{d_i}$ , is also small as compared with the system size  $N$ . This implies that the possibility that an oscillator at a small distance  $d_i$  is also connected by a path of length slightly larger than  $d_i$  can be neglected. Consequently, for oscillators at small distances from the node at which the perturbation is applied, the sum in the second line of Eq. (15) is dominated by the term with  $m = d_i$ . This dominance is enhanced for large  $|z + i\Omega|$ , because successive terms in the sum are weighted by increasing inverse powers of that number. If the system is large enough we can drop the last term in the second line of Eq. (15), and write  $A_i \approx (z + i\Omega)^{-d_i - 1}$ , i. e.

$$A_i \approx (z^2 + \Omega^2)^{-\frac{d_i+1}{2}} \exp \left[ -i(d_i + 1) \tan^{-1} \frac{\Omega}{z} \right]. \quad (16)$$

Within this approximation, the small-distance exponential dependence of the amplitude modulus,  $|A_i| \approx (z^2 + \Omega^2)^{-\frac{d_i+1}{2}}$  is apparent. Straight lines in Fig. (6) show the excellent agreement between the predicted slope of  $|A_i|$  and our numerical results. Equation (16) also explains the linear dependence of the phase shift  $\varphi_i$  with the distance. Specifically, it predicts a unitary phase shift  $\Delta\varphi = -\tan^{-1}(\Omega/z)$ . Straight lines in Fig. 7 stand for this prediction.

Two effects contribute to break down the small-distance approximation (16). First, as discussed above, we expect that this approximation does not hold beyond dis-

tances where  $z^{d_i} \sim N$ , i. e.  $d_i \sim \log N / \log z$ . At larger distances, in fact, it is not true that only one path contributes to the propagation of the perturbation signal from the node at which it is applied. The second effect has to do with the relative magnitude of the first non-zero term in the sum of the last line of Eq. (15) and the term of order  $N^{-1}$ . For sufficiently large distances, the latter cannot be neglected with respect to the former. If  $\Omega \ll z$ , the two terms become comparable for  $z^{d_i+1} \sim N\Omega$ , while if  $z \ll \Omega$  they are similar for  $\Omega^{d_i} \sim N$ . It turns out that, in both limits, this second effect acts at distances smaller than the first one. This does not imply, however, that the first effect plays no role in determining the response of the system at large distances.

It can be shown that, for oscillators at large distances from oscillator 1, the matrix element in the sum of Eq. (15) can be accurately approximated as  $J_{i1}^{(m)} = J_0 z^m$  for all  $m \geq d_i$ , while  $J_{i1}^{(m)} = 0$  for  $m < d_i$ . In fact, we can argue that the number of paths of length  $m$  ending at a given oscillator  $i$  scales as  $z^m$  for large  $m$ , by noticing that this number is  $z$  times the number of paths of length  $m-1$  ending at the oscillators to which  $i$  is coupled. The precise value of the prefactor  $J_0$  depends on  $N$  and on the specific realization of the network, but is independent of the distance  $d_i$ . For the network corresponding to the numerical results presented above, for instance,  $J_0 \approx 9.91 \times 10^{-4}$ .

Replacing the *Ansatz* for  $J_{i1}^{(m)}$  in Eq. (15) and performing the summation, we get

$$A_i \approx \frac{i}{\Omega} \left[ -J_0 \left( 1 + \frac{\Omega^2}{z^2} \right)^{-\frac{d_i}{2}} \exp \left( -id_i \tan^{-1} \frac{\Omega}{z} \right) + \frac{1}{N} \right]. \quad (17)$$

This large-distance approximation for the complex amplitude  $A_i$  is more clearly analyzed for limit values of the frequency  $\Omega$ . For small  $\Omega$ , specifically for  $d_i \Omega / z \ll 1$ , the amplitude modulus is

$$|A_i| \approx \frac{1}{\Omega} \sqrt{\frac{d_i^2 \Omega^2}{z^2} J_0^2 + \left( \frac{1}{N} - J_0 \right)^2}. \quad (18)$$

As found in our numerical results, Figs. (1) and (6), the response grows with  $d_i$  for large distances. Combined with the decrease observed for small distances, this explains the existence of an intermediate minimum in both  $|A_i|$  and  $\sigma_\phi$ .

The amplitude phase

$$\varphi_i = -\tan^{-1} \frac{z}{d_i \Omega} \left( \frac{1}{J_0 N} - 1 \right) \quad (19)$$

exhibits a more complicated functional dependence with the distance. In the opposite limit of large frequencies, the large-distance approximation (17) is dominated by the last term,  $A_i \approx i/N\Omega$ . We recall that this term stands for the contribution of the average deviation from full synchronization to the individual motion of oscillators. The amplitude modulus becomes independent of the distance, as found in the results of Fig. 6. Its phase is always  $\pi/2$  –or, more generally,  $\pi/2 + 2k\pi$ , with  $k$  an integer. In the results for large  $\Omega$  shown in Fig. 7, we have  $\varphi \approx \pi/2 - 2\pi \approx -4.71$ .

Coming back to the full form of our approximation for the amplitude, Eq. (15), let us finally point out that, for sufficiently large frequency  $\Omega$  and irrespectively of the distance  $d_i$ , the dominant terms are of order  $\Omega^{-1}$ . To this order, the sum contributes its first term,  $m = 0$ . Since

$\mathcal{J}^0 = \mathcal{I}$ , for  $\Omega \rightarrow \infty$  we get

$$A_i \approx \frac{i}{\Omega} \left( -\delta_{i1} + \frac{1}{N} \right). \quad (20)$$

This result explains the decay as  $\Omega^{-1}$  in the tails of the resonance peaks, displayed in Fig. 3. It also shows that the large-frequency response of oscillator 1 is  $N$  times larger than that of any other oscillator, as illustrated in the same figure. Moreover, we find that the phase shift of oscillator 1 is  $\varphi_1 = -\pi/2$  while any other oscillator is dephased by  $\pi/2$  with respect to the external perturbation.

## 4 Extensions

### 4.1 Other regular network structures

It is important to remark that the analytical approach presented in Sect. 3, so far applied to random networks, is valid for a large class of interaction patterns. In fact, the only condition imposed on the adjacency matrix  $\mathcal{J}$  to obtain the results of Sect. 3.1 is that  $\sum_j J_{ij} = z$  for all  $i$ , while the approximation of Sect. 3.2 requires that  $\sum_i J_{ij} \approx z$  for all  $j$ . These conditions imply, respectively, that each oscillator is coupled to exactly  $z$  neighbours and that, in turn, the number of oscillators coupled to each oscillator is also approximately constant. Under such conditions, our approach can be used to evaluate the response of an ensemble with any interaction pattern. In this section, we illustrate this fact with a few cases that admit to be worked out explicitly.

Consider first a linear array of  $N$  oscillators with periodic boundary conditions, where each oscillator is coupled to its nearest neighbour to the left ( $z = 1$ ). We assume that oscillators are numbered from left to right in the natural order. For this directed ring, we have  $J_{ij} = 1$  if

$i = (j + 1) \bmod N$ , and  $J_{ij} = 0$  otherwise. Consequently,  $\sum_k J_{kj} = 1$  for all  $j$ , and the approximation of Sect. 3.2 is exact. The relevant elements of  $\mathcal{J}^m$  are  $J_{i1}^{(m)} = 1$  if  $m = d_i + kN$  ( $k = 0, 1, 2, \dots$ ), and  $J_{i1}^{(m)} = 0$  otherwise. In fact, the only paths that join oscillator 1 with oscillator  $i$ , at distance  $d_i = i - 1$ , are those of length  $d_i$  plus an integer number  $k$  of turns around the ring. The calculation of the amplitudes yields

$$A_i = \frac{(1 + i\Omega)^{-d_i - 1}}{1 - (1 + i\Omega)^{-N}} + \frac{i}{N\Omega}. \quad (21)$$

For  $\Omega \ll 1$ , but with  $N\Omega \gg 1$ , the amplitude at essentially all distances ( $d_i \lesssim N$ ) is dominated by the first term of Eq. 21. In this regime,  $|A_i|$  decreases exponentially with  $d_i$  and the phase shift  $\varphi_i$  varies linearly, with  $\Delta\varphi = -\tan^{-1} \Omega$ . In the opposite limit of large frequencies,  $\Omega \gg 1$ , the amplitude decays as  $\Omega^{-1}$ . For oscillator 1 ( $d_1 = 0$ ), we have  $A_1 \approx -i/\Omega$ , while for any other oscillator ( $d_i > 0$ ),  $A_i \approx i/N\Omega$ . We stress the qualitative similarity between these results and those obtained for random networks.

Note that in the limit  $N \rightarrow \infty$ , the perturbation cannot attain the oscillators to the left of oscillator 1, and there is only one path (of length  $m = d_i$ ) for the signal to reach the oscillators to its right. In this limit,  $A_i = (1 + i\Omega)^{-d_i - 1}$  at all distances, and the regime of exponential decay and linear phase shift extends over the whole system to the right of the node where the perturbation is applied.

Consider now a linear array –which, for simplicity, we treat in the limit  $N \rightarrow \infty$ – where each oscillator is coupled to its two first neighbours ( $z = 2$ ). Again, the approximation of Sect. 3.2 is exact. With this bidirectional

coupling, there are infinitely many directed paths joining any two nodes in the network. A path of length  $m$  between oscillator 1 and oscillator  $i$  consists of  $m_+$  steps to the right and  $m_-$  steps to the left, with  $m_+ + m_- = m$  and  $|m_+ - m_-| = d_i$ . The number of such paths is

$$J_{i1}^{(m)} = \binom{m}{m_+} = \binom{m}{\frac{m+d_i}{2}} \quad (22)$$

if  $m$  and  $d_i$  ( $m \geq d_i$ ) are both even or odd, and 0 otherwise. To perform the summation in Eq. (15), it is convenient to write  $m = d_i + 2q$  and sum over  $q = 0, 1, \dots$ . This yields

$$\begin{aligned} A_i &= \sum_{q=0}^{\infty} \frac{\binom{d_i + 2q}{q}}{(2 + i\Omega)^{d_i + 2q + 1}} \\ &= \frac{{}_2F_1\left[\frac{d_i+1}{2}, \frac{d_i}{2} + 1; d_i + 1; \frac{4}{(2+i\Omega)^2}\right]}{(2 + i\Omega)^{d_i+1}}, \end{aligned} \quad (23)$$

where  ${}_2F_1(a, b; c; z)$  is the hypergeometric function [24]. This exact result can be approximately analyzed for limiting values of  $\Omega$ . For  $\Omega \ll 1$ , the amplitude modulus decreases exponentially with the distance, as  $|A_i| \propto (1 + \sqrt{2\Omega})^{-d_i/2}$ , while the phase shift varies linearly with  $d_i$ , with slope  $\Delta\varphi = -\tan^{-1}(1 + \sqrt{2/\Omega})^{-1}$ . Note that the exponential decrease of  $|A_i|$  is much slower than in the case of random networks with the same  $z$ . For random networks, in fact, we have found that—in the limit of small frequency and in the regime of exponential decay— $|A_i| \sim z^{-d_i-1}$ . Here, on the other hand, the decay of  $|A_i|$  becomes increasingly slower as  $\Omega \rightarrow 0$ . This important difference is a consequence of the fact that, in a random network and at small distances, essentially only one path

contributes to the propagation of the perturbation signal towards each oscillator. For the bidirectional linear array, in contrast, the total number of paths  $\sum_m J_{i1}^{(m)}$  grows exponentially with  $d_i$ . This growth compensates partially the exponentially decreasing contributions from successive path lengths [cf. Eq. (15)].

In the limit of large frequency, on the other hand, we find  $A_i \approx (2 + i\Omega)^{-d_i-1}$ , i. e.  $|A_i| \sim \Omega^{-d_i-1}$ . It is essential to this result, however, that—assuming an infinitely large system—we have neglected the term of order  $N^{-1}$  in Eq. (15). For any finite size, if  $N$  is fixed, the limit of large frequencies is dominated by this term, and  $|A_i| \sim \Omega^{-1}$ .

Let us finally consider a interaction network with a hierarchical structure, in the form of a directed tree where nodes are distributed into successive layers. An oscillator at a given layer is coupled to only one oscillator in the layer immediately above, so that  $z = 1$ , and the uppermost layer consists of a single oscillator, where the external perturbation is applied. Thus, the perturbation propagates downwards through the hierarchy. If layers are labeled in the natural order starting by  $l = 0$  at the uppermost layer, the distance  $d_i$  of any oscillator to the node where the perturbation is applied coincides with the label of its layer. Namely, oscillators at level  $l = 1$  have  $d_i = 1$ , at level  $l = 2$  they have  $d_i = 2$ , and so on. There is only one path, of length  $d_i$ , through which the perturbation can reach oscillator  $i$ . Therefore, only one term contributes to the sum in Eq. (15). Now, it is important to note that the approximation (ii) introduced in Sect. 3.2 is no longer suitable. While each oscillator is coupled to only one neighbour,

the number of oscillators coupled to oscillator  $j$ ,  $\sum_k J_{kj}$ , is typically larger than one. In a regular hierarchical structure, in fact, we fix  $\sum_k J_{kj} = z' > 1$  for all  $j$ . In this situation, Eq. (15) changes in such a way that the last term becomes multiplied by a factor  $z'/z$ . The amplitude is

$$A_i = (1 + i\Omega)^{-d_i - 1} + \frac{z'}{z} \frac{i}{N\Omega}. \quad (24)$$

Not unexpectedly, this result is similar to that for a unidirectional linear array, Eq. (21). In the first term, which stands for the exponential-decay regime, the main difference corresponds to a factor which, in the case of the array, takes into account that the perturbation signal reaches an oscillator at each turn around the array. In the second term, the two results differ precisely in the factor  $z'/z$ . This effect enhances the response of oscillators with  $d_i > 0$  at large frequencies, where  $|A_i| \approx z'/zN\Omega$ .

## 4.2 Non-regular random networks

So far, our numerical and theoretical analyses have dealt with regular networks, where all oscillators are coupled to exactly the same number  $z$  of neighbours. While the analytical approach cannot be extended to the case of more general structures, it is worthwhile to show that our results hold—at least, qualitatively—for non-regular random networks. For sufficiently large networks, with a well defined average number of neighbours per site, it is in fact expected that statistical quantities such as the mean square deviation  $\sigma_{\phi_i}$  are essentially not sensible to the regularity of the interaction pattern.

We consider non-regular random networks of two types. In the first type (random I) the number of neighbours  $z_i$  of each site  $i$  is chosen to be 1, 2 or 3 with equal probability  $1/3$ . The average number of neighbours is thus  $\bar{z} = 2$ , which makes it possible to compare with our results for regular networks with  $z = 2$ . Once  $z_i$  has been defined, the neighbours of site  $i$  are chosen at random from the whole system, avoiding self-connections and multiple connections. In the second type of non-regular random networks (random II), the number of neighbours of each site is drawn from the discrete probability distribution  $p(z) = 2^{-z}$  ( $z = 1, 2, \dots$ ), which also insures  $\bar{z} = 2$  but with a much wider dispersion. Our numerical calculations were run for a system of  $N = 10^3$  oscillators, with a perturbation amplitude  $a = 10^{-3}$ .

Figure 8 shows results for the mean square deviation from full synchronization  $\sigma_{\phi}$ , with the two types of non-regular random networks. For the sake of comparison with the case of regular networks, the perturbation frequencies  $\Omega$  are the same as in Fig. 1. Moreover, specific realizations of the networks with the same maximal distance to the perturbed oscillator,  $d_{\max} = 15$ , were selected. The vertical axes cover also the same range. We verify at once that the main features in the dependence of the mean square deviation on the distance found for regular interaction patterns are also present in non-regular networks. As it may have been expected, quantitative differences are more important for small frequencies, i.e. near the resonance. There, the oscillator network is more sensible to the perturbation and, arguably, its detailed structure plays a

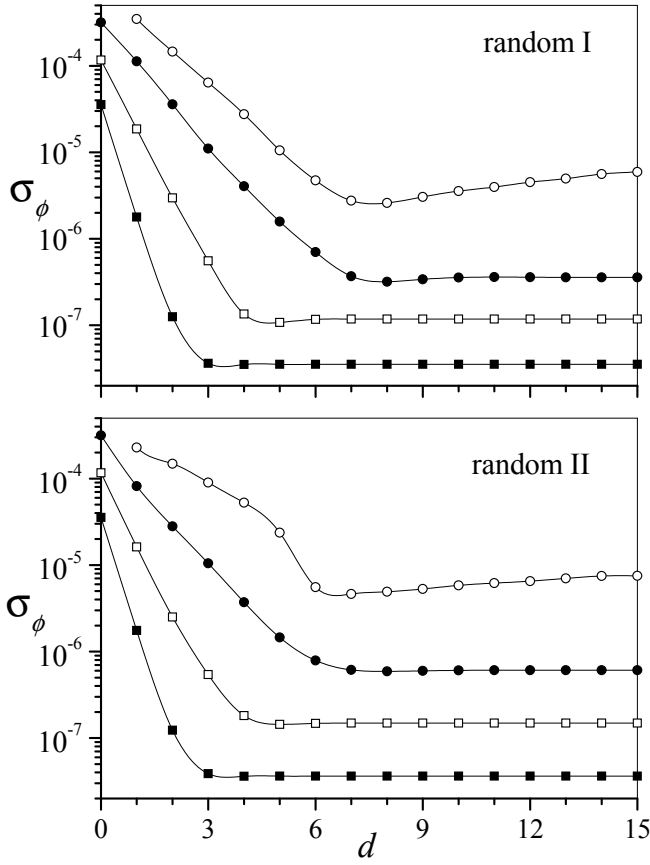


**Fig. 8.** Mean square deviation from full synchronization in non-regular random oscillator networks of the two types described in the text (random I and II), for various values of the perturbation frequency  $\Omega$ . Symbols are as in Fig. 1.

more noticeable role in determining its response. For larger frequencies, the values of  $\sigma_\phi$  become increasingly indistinguishable from those obtained for regular networks.

### 4.3 Chaotic oscillators

An important question regarding the generality of the results presented so far is whether they apply to ensembles of coupled elements whose individual dynamics are not simple phase oscillations. While we may argue that any cyclic behaviour, even in the presence of external forces,

can be approximately described by a periodic phase oscillator [9], the question remains open for chaotic coupled dynamical systems. To address this problem we have considered an ensemble of Rössler oscillators, described by the equations

$$\dot{x}_i = -y_i - z_i + k \sum_j J_{ij}(x_j - x_i) + a\delta_{i1} \sin \Omega t$$

$$\dot{y}_i = x_i + 0.2y_i + k \sum_j J_{ij}(y_j - y_i) \quad (25)$$

$$\dot{z}_i = 0.2 + z_i(x_i - c) + k \sum_j J_{ij}(z_j - z_i).$$

The parameter  $c$  controls the nature of the oscillations; for  $c = 4.46$  they are chaotic [22]. As in Sects. 2 and 3, we choose the adjacency matrix such that  $\sum_j J_{ij} = z$  for all  $i$ . Each Rössler oscillator is thus coupled to exactly  $z$  neighbours. Chaotic systems can be fully synchronized if the coupling intensity  $k$  is larger than a certain threshold value, related to the Lyapunov exponent of the individual dynamics [2,11]. For the above value of  $c$ , a coupling intensity  $k = 0.2$  insures that full synchronization is stable. In our ensemble of Rössler oscillators, the external perturbation acts on just one of the coordinates of oscillator 1, namely, on  $x_1(t)$ .

The numerical results presented below have been obtained for an ensemble of  $N = 10^3$  Rössler oscillators, with  $z = 2$  and the parameters quoted in the preceding paragraph. For the sake of comparison, the interaction network is the same as in our study of phase oscillators (Sects. 2 and 3). The amplitude of the external perturbation is  $a = 10^{-3}$ . As a characterization of the response of the system, we have used a natural extension of the

mean square deviation from full synchronization defined in Eq. (3) for phase oscillators, given by

$$\sigma_{\mathbf{r}_i} = (\langle |\mathbf{r}_i - \bar{\mathbf{r}}|^2 \rangle)^{1/2}, \quad (26)$$

with  $\mathbf{r}_i = (x_i, y_i, z_i)$  and  $\bar{\mathbf{r}} = N^{-1} \sum_i \mathbf{r}_i$ . Time averages, indicated as  $\langle \cdot \rangle$ , are performed over sufficiently long intervals, after transients have been left to elapse. Figure 9 shows numerical results for the mean square deviation as a function of the distance, and for various perturbation frequencies. Individual values of  $\sigma_{\mathbf{r}_i}$  for Rössler oscillators at a given distance from oscillator 1 have been averaged, and the index  $i$  has been dropped accordingly. We see that the overall behaviour of  $\sigma_{\mathbf{r}}$  as a function of  $d$  is similar to that found for ensembles of phase oscillators (cf. Fig. 1), with rapid decrease for small distances and smooth growth for large distances. In all cases, the two regimes are separated by a well defined minimum. The exponential character of the decrease for small  $d$  and the saturation of  $\sigma_{\mathbf{r}}$  for large  $d$  are, however, much less clear than for phase oscillators.

The results of Fig. 9 clearly show that the mean square deviation varies non-monotonically with the perturbation frequency. The dependence of  $\sigma_{\mathbf{r}}$  with  $\Omega$  is expected to reveal the resonance nature of the system response. The natural frequency  $\omega$  of individual Rössler oscillators can be defined, in the chaotic regime, in terms of the average period  $T$  of the chaotic oscillations. Each period is determined, for instance, as the time needed for an oscillator to cross the plane  $y = 0$  in the subspace  $x < 0$ . These times are then averaged over a large number of oscillations, and the frequency is calculated as  $\omega = 2\pi/T$ . For  $c = 4.46$ , we find  $\omega \approx 1.08$ .

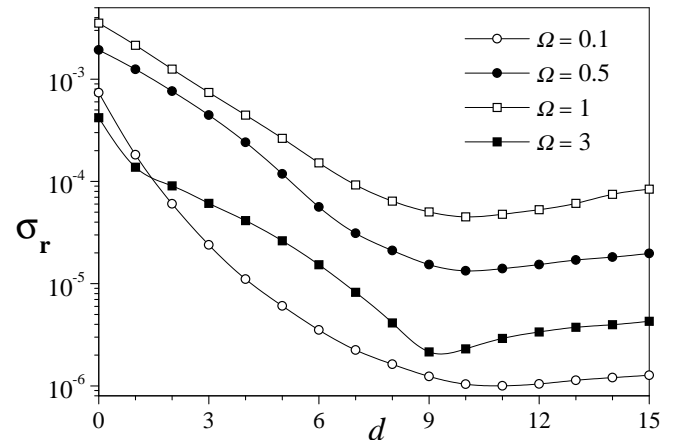


**Fig. 9.** Mean square deviation from full synchronization as a function of the distance for an ensemble of Rössler oscillators, for various values of the frequency  $\Omega$ . Spline interpolations are shown as curves.

In Fig. 10 we present numerical results for the mean square deviation from full synchronization as a function of  $\Omega$ , for several distances. For  $d = 0$ , we find the expected resonance maximum at  $\Omega \approx \omega$ . Interestingly enough, there is an additional local maximum at  $\Omega \approx 2\omega$ , corresponding to a harmonic resonance induced by non-linear effects. The presence of this extra peak is consistent with the fact that higher-harmonic components are very relevant contributions to the chaotic motion of individual Rössler oscillators [23]. For larger distances, the resonance maximum is replaced by a double peak, as we have found for phase oscillators (Fig. 2), with a relative minimum at  $\Omega \approx \omega$  and two lateral maxima. At the site of the harmonic resonance we find the same structure. In contrast with the case of phase oscillators, however, the double peak persists at large distances, with better defined maxima as  $d$  grows.



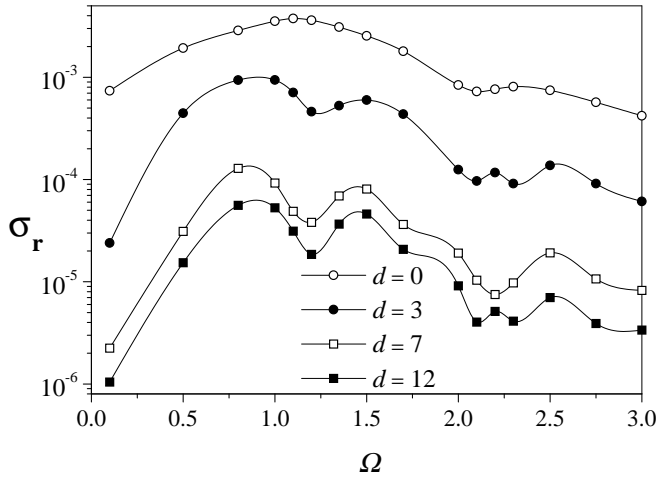


**Fig. 10.** Mean square deviation from full synchronization as a function of perturbation frequency for an ensemble of Rössler oscillators, at various distances from the node where the perturbation is applied. Spline interpolations are shown as curves.

We have also verified that, as for phase oscillators, the individual motions of Rössler oscillators at the same distance from oscillator 1 are in-phase. These coherent dynamics give rise to a clustered distribution in  $\mathbf{r}$ -space, and a snapshot of the ensemble in that space produces a picture qualitatively very similar to Fig. 4.

## 5 Discussion and conclusion

In this paper, we have studied the response of an ensemble of fully synchronized oscillators to an external perturbation. The perturbation is represented as an additional oscillator, evolving autonomously with a fixed frequency. One of the oscillators of the ensemble is coupled to this additional element. The perturbation propagates through the system due to the coupling between oscillators. In the absence of the external action, this interaction sustains

the state of full synchronization. The system can thus be thought of as an active extended medium with a highly coherent rest state –full synchronization– whose response to the external perturbation is driven by the collective dynamics of the interacting oscillators. Such response, in fact, provides a characterization of the collective dynamics.

Our study was mainly focused on ensembles of identical phase oscillators. In its usual formulation, Kuramoto’s model considers global coupling, where interactions are identical for all oscillator pairs. In this situation, all oscillators are mutually equivalent, and the response to the external perturbation –other than on the oscillator where the perturbation is applied– is homogeneous over the whole system. Therefore, we have considered more complex interaction patterns, introducing interaction networks which allow for a non-trivial distribution of distances between oscillators. Interactions were not necessarily bidirectional, so that coupling was not always symmetric. To take advantage of certain analytical results on the stability of full synchronization [11], we have considered regular networks, where all oscillators are coupled to the same number of neighbours. Numerical results obtained show, however, that this choice does not represent a strong restriction on the interaction network. The number of neighbours of each oscillator and the frequency of the external perturbation are the main parameters that control the response of the system.

For moderate values of its amplitude, the external perturbation induces oscillations around the state of full syn-

chronization. Our main conclusion, first found by numerical means, is that the response of each individual oscillator exhibits a clear dependence on the distance from the node where the perturbation is applied. For random interaction networks, this dependence shows two well defined regimes. At small distances, the amplitude of the individual oscillations decreases exponentially with the distance. Meanwhile, the phase shift of these oscillations with respect to the external perturbation, which measures the delay of the individual response, varies linearly with the distance. In this regime, thus, the perturbation propagates through the system at constant velocity, and is progressively damped at a rate proportional to its own amplitude. In other words, the system behaves as a linear dissipative medium. For large distances, on the other hand, the individual response saturates and the dependence of the amplitude and the phase shift with the distance becomes much smoother. The relative extension of the two regimes, as well as the rates of attenuation and dephasing of the perturbation signal in the linear regime, depend on the frequency of the external perturbation and on the number of neighbours of each node.

The fact that the phase shift of individual oscillations with respect to the external perturbation is defined by the distance to the node where the perturbation is applied, implies that all the oscillators at a given distance respond to the perturbation coherently. Since the amplitudes of their oscillations are also similar, the “spatial” distribution of the ensemble –i.e. the distribution in the relevant one-particle state space– becomes clustered. Especially in

the small-distance regime, where the individual response strongly depends on the distance, all the oscillators at a given distance form a compact cluster with coherent oscillatory motion. Thus, the external perturbation induces a “spatial” organization associated with the internal structure of the interaction network.

The overall response of the system to the external perturbation is maximal when the perturbation frequency is equal to the natural frequency of the oscillators. This not unexpected resonance phenomenon is revealed by the presence of a peak in the amplitude of individual oscillations as a function of the perturbation frequency. Far from the peak, the amplitude decreases as the inverse of this frequency. For oscillators at intermediate distances, however, an anomaly in the response appears. The resonance peak is replaced by a double peak, with a minimum at the resonance frequency and two lateral maxima. As we discuss below, this effect can be interpreted as an interference phenomenon.

Our numerical results are well reproduced by an analytical approach based on a linear approximation for small perturbation amplitudes. This approach is able to discern between the roles of different contributions to the response of the system. Two complementary aspects are worth mentioning. First, we have found that the existence of two regimes in the distance dependence is directly associated with the distribution of the number of paths in the interaction network. The perturbation signal reaches oscillators at small distances essentially through only one path. The dissipative mechanisms inherent to the dynam-

ics of the oscillator ensemble progressively attenuates the signal, which decays exponentially with the distance. For oscillators at large distances, on the other hand, the number of available paths grows exponentially, at a rate that—at least, for small perturbation frequencies—is similar to the rate of exponential decay of the signal. These two partially compensating effects determine that the variation of the response with the distance is much smoother for large distances.

The second aspect has to do with the fact that the external perturbation affects individual oscillators in two ways. Besides the propagation of the signal through the network, which acts on the oscillators with different intensities depending on their distance to the node where the perturbation is applied, there is an overall contribution originated by the average motion of the whole ensemble, which affects all oscillators with the same intensity. This global contribution is inversely proportional to the system size, and therefore could be generally neglected for sufficiently large systems. However, it does play an important role in determining the system response at distances where the propagating signal has been strongly damped. It also determines the response at high perturbation frequencies, where the propagation mechanism is very ineffective, especially, at large distances. Our analysis shows that the overall contribution of the average motion of the ensemble and the local contribution of the propagated signal have opposite signs. In other words, their oscillation phases differ by  $\pi$ , in such a way that, if their amplitudes are similar, a phenomenon of destructive interference takes place. In

our random networks this happens, precisely, at the transition between the two regimes discussed above, when the amplitude response has decreased by a factor of about the inverse of the system size. The minimum in the amplitude at those intermediate distances can thus be interpreted as the result of the destructive interference between the two contributions that affect individual motions.

Generally, we may expect that interference phenomena play an important role in the dynamics of oscillator networks. This is due to the fact that, as we have seen, the oscillatory signal changes its phase as it propagates through the network. The signal can reach a given oscillator through different paths, and thus with different phases. The sum of all those contributions will depend not only on their amplitudes but also on their relative dephasing, likely giving rise to interference. From this perspective, the saturation of the response at large distances, where contributions from many different paths are acting, could be interpreted as a phenomenon of constructive interference that breaks down the regime of exponential decay.

The applicability of our analytical approach is not restricted to random networks. We have shown how our main results extend to regular and hierarchical arrays of phase oscillators. Numerical calculations show, moreover, that the same results are qualitatively reproduced in non-regular random interaction patterns. The most important extension considered here, however, has consisted of replacing phase oscillators by chaotic Rössler oscillators. The response of ensembles of these chaotic elements to the external perturbation was analyzed by numerical means.

In spite of the essential difference in the nature of the individual dynamics, we have verified that the most important features found for phase oscillators are qualitatively reproduced by Rössler oscillators. Specifically, the existence of two regimes, depending on the distance to the oscillator where the external perturbation is applied, and the resonance nature of the response are also observed for the chaotic elements. Non-linearities inherent to the chaotic dynamics contribute extra effects, such as higher-harmonic resonances.

As a concluding remark, let us stress that our analysis establishes a close connection between the collective dynamics of an ensemble of coupled oscillators subject to an external action and the interaction pattern underlying the ensemble. This connection provides a method to indirectly infer the structure of such interaction pattern by studying the response of individual oscillators to an external perturbation. Sampling the motion induced by a perturbation applied at different nodes on various oscillators may be used as an experimental tool to reconstruct the interaction network.

## References

1. A. S. Pikovsky, M. Rosenblum, and J. Kurths, *Synchronization. A Universal Concept in Non-linear Sciences* (Cambridge University Press, Cambridge, 2001).
2. S. C. Manrubia, A. S. Mikhailov, and D. H. Zanette, *Emergence of Dynamical Order. Synchronization Phenomena in Complex Systems* (World Scientific, Singapore, 2004).
3. H. Strogatz and I. Stewart, *Sci. Am.* **269** (1993) 102-115.
4. G. D. VanWiggeren and R. Roy, *Science* **279** (1988) 1198-1200.
5. I. Z. Kiss, Y. Zhai, and J. L. Hudson, *Science* **296** (2002) 1676-1678.
6. J. Buck and E. Buck, *Sci. Am.* **234** (1976) 74-85.
7. A. T. Winfree, *The Geometry of Biological Time* (Springer, New York, 2001).
8. C. M. Gray, P. König, A. K. Engel, and W. Singer, *Nature* **338** (1989) 334-337.
9. Y. Kuramoto, *Chemical Oscillations, Waves, and Turbulence* (Springer, Berlin, 1984).
10. S. Boccaletti, J. Kurths, G. Osipov, D. L. Valladares, and C. S. Zhou, *Phys. Rep.* **366** (2002) 1-101.
11. M. G. Earl and S. H. Strogatz, *Phys. Rev. E* **67** (2003) 036204.
12. H. Daido, *Prog. Theor. Phys.* **77** (1987) 622-634.
13. A. T. Winfree, *J. Theor. Biol.* **16** (1967) 15-42.
14. H. Sakaguchi, *Prog. Theor. Phys.* **79** (1988) 39-46.
15. K. Kaneko, *Phys. Rev. Lett.* **63** (1989) 219-223.
16. N. Nakagawa and Y. Kuramoto, *Prog. Theor. Phys.* **89** (1993) 313-323.
17. G. Veser, F. Mertens, A. S. Mikhailov, and R. Imbühl, *Phys. Rev. Lett.* **71** (1993) 935-939.
18. P. Coulet and K. Emilsson, *Physica D* **61** (1992) 119-131.
19. H. Kori and A. S. Mikhailov, *Pacemakers in randomly coupled oscillator networks*, cond-mat/0402519.
20. D. H. Zanette, *Propagation of small perturbations in synchronized oscillator networks*, cond-mat/0409159.
21. J. Gross and J. Yellen, *Graph Theory and its Applications* (CRC Press, Boca Raton, 1999).
22. A. S. Mikhailov and A. Yu. Loskutov, *Foundations of Synergetics II* (Springer, Berlin, 1991).

23. P. G. Drazin, *Nonlinear Systems* (Cambridge University Press, Cambridge, 1994).
24. M. Abramowitz and I. A. Stegun, *Handbook of Mathematical Functions* (Dover, New York, 1972).